Nucleic Acids Research, 1998, Vol. 26, No. 19 **4315–4323**

Synthesis and pairing properties of oligoribonucleotide analogues containing a metal-binding site attached to β-D-allofuranosyl cytosine

Xiaolin Wu and Stefan Pitsch*

Organisch-Chemisches Laboratorium der Eidgenössischen Technischen Hochschule, Universitätstrasse 16, CH-8092 Zürich, Switzerland

Received July 22, 1998; Revised and Accepted August 18, 1998

ABSTRACT

A method for the facile preparation of oligoribonucleotide analogues containing β-D-allofuranosyl nucleosides with additional functional groups tethered to the 6′-*O* positions is presented. It is based on the synthesis of two protected nucleosides carrying a 6′-*O*-bromopentyl and a 6′-*O*-methylaminopentyl substituent. By a simple two-step procedure, these key intermediates were transformed into two phosphoramidites carrying a 1-aza-18-crown-6 and a triethyleneglycol group, respectively, each capable of complexing metal ions. By automated synthesis, these functionalized nucleoside analogues were efficiently incorporated into short oligoribonucleotides. Under physiological conditions (150 mM NaCl, 2 mM $MgCl_2$, pH 7.4), incorporation of a single allofuranosyl cytosine substituted with a triethyleneglycol moiety led to a significant enthalpic stabilization of an A-type RNA duplex. This observation is in agreement with a metal ion-mediated stabilizing interaction between the two pairing strands.

INTRODUCTION

Modified and functionalized oligonucleotides play an important role as molecular tools and potential antisense drugs (1). Furthermore, there exists an as yet unexploited potential for catalysis of chemical reactions with tailored ribozymes containing additional side chains (2). So far, oligonucleotides have been functionalized at the nucleobases, at the 5′- or 3′-termini, at the phosphodiester linkages or at the 2′-*O* position (for recent examples see 3–6).

During our ongoing investigations of the properties of hexofuranosyl oligonucleotides we developed a method for the synthesis of oligoribonucleotides containing 6′-*O*-substituted β-D-allofuranosyl and β-L-talofuranosyl nucleosides, which can be regarded as C(5′)-substituted ribonucleosides. Preliminary melting curve studies revealed that single incorporations of D-allofuranosyl nucleosides in an A-type RNA duplex did not significantly change the pairing properties (relative to those of the parent duplex), whereas incorporation of [the C(5′)-epimeric] L-talofuranosyl nucleosides resulted in substantial weakening of the duplex (7; X.Wu, unpublished results).

Here we present a synthesis of the two β-D-allofuranosyl cytosine building blocks **9** and **13**, containing all protecting groups required for automated synthesis and a 6′-*O*-bromopentyl (electrophilic) or a 6′-*O*-methylaminopentyl (nucleophilic) substituent, respectively. The 2′-*O* positions were protected with the $Pr^i_3SiOCH_2$ (TOM) group, which we recently introduced for the chemical synthesis of oligoribonucleotides under standard DNA coupling conditions (8; S.Pitsch, X.Wu, P.A.Weiss, S.Vonhoff and L.Jenny, in preparation).

The two reactive building blocks **9** and **13** potentially serve as starting materials for a variety of functionalized oligoribonucleotide analogues, allowing the straightforward introduction of different side chains at a very late stage of monomer synthesis. As first examples, we functionalized them with two metal chelating moieties and transformed them into phosphoramidites **15** and **17**. Preliminary molecular model studies indicated the possibility of an interaction between a tethered metal complex (covalently bound to the 6′-*O* position of an allofuranosyl nucleoside) and the phosphodiester backbone of an unmodified partner strand across the major groove. When an appropriate alignment is realized, such an interaction can potentially stabilize the duplex electrostatically or catalyse a specific strand scission reaction by providing a correctly positioned Lewis acid. Triethyleneglycol and 1-aza-18-crown-6 were chosen as ligands for their known ability to form complexes with the biologically abundant metal ions Na^+, K^+, Mg^{2+} and Ca^{2+} (9,10).

RESULTS

Synthesis of monomers

For synthesis of the key intermediates **9** and **13** we first prepared the appropriately pre-functionalized sugar building blocks **3** and **4** which allowed an efficient, stepwise introduction of the nucleobase, the dimethoxytrityl group and the 2′-*O* protecting group (Scheme 1).

Selective alkylation of the primary hydroxy group in diol **1** (11) with 1,5-dibromopentane gave bromide **2** in good yields. This reaction was accomplished by first forming the cyclic dibutyl tin-derivative, followed by alkylation in the presence of tetrabutylammonium iodide and caesium fluoride according to Nagashima and Ohno (12). The common precursor **2** could be elaborated by a series of reactions into sugar building blocks **3** and **4** without intermediate purification. The bromopentyl sugar **3** was obtained by

*To whom correspondence should be addressed. Tel: +41 1 632 4481; Fax: +41 1 632 1136; Email: pitsch@xeragon.com

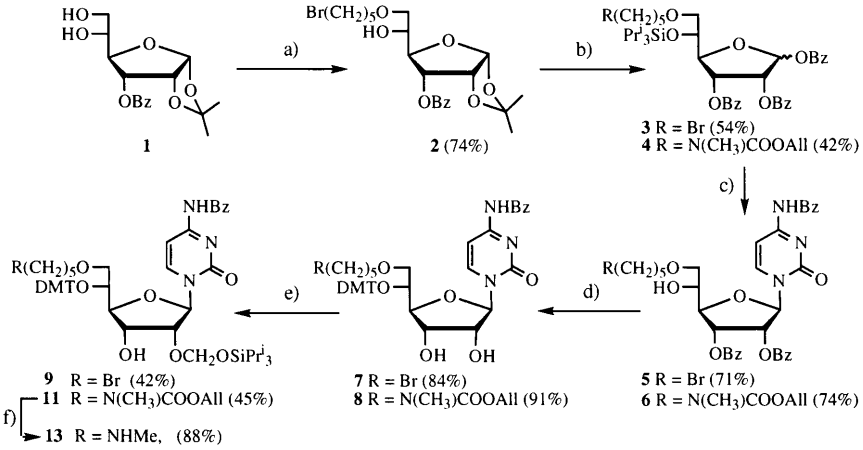

Scheme 1. Reagents and conditions. (a) (i) Bu_2SnO, toluene, reflux, (ii) $Br(CH_2)_5Br$, CsF, Bu_4NI, DMF, room temperature. (b) For **3**: (i) Pr^i_3Si–OTf, $Et(Pr^i)_2N$, CH_2Cl_2, room temperature, (ii) CF_3COOH, H_2O, room temperature, (iii) BzCl, DMAP, py, CH_2Cl_2, room temperature; for **4**: (i) Pr^i_3Si–OTf, $Et(Pr^i)_2N$, CH_2Cl_2, room temperature, (ii) $MeNH_2$, EtOH, room temperature, (iii) AllOC(O)Cl, $Et(Pr^i)_2N$, CH_2Cl_2, room temperature, (iv) CF_3COOH, H_2O, room temperature, (v) BzCl, DMAP, py, CH_2Cl_2, room temperature. (c) (i) Bis(trimethylsilyl)acetamide, N^4–benzoylcytosine, MeCN, 70°C, then Me_3Si–OTf, (ii) HF, HCl, MeCN, room temperature; (d) (i) DMT–Cl, $AgNO_3$, *sym*–collidine, CH_2Cl_2, room temperature, (ii) NaOH, THF/MeOH/H_2O, 4°C. (e) Bu_2SnCl_2, Pr^i_3Si–OCH_2Cl, $Et(Pr^i)_2N$, $(CH_2Cl)_2$, 70°C. (f) $Pd(PPh_3)_4$, Et_2NH, PPh_3, CH_2Cl_2, room temperature.

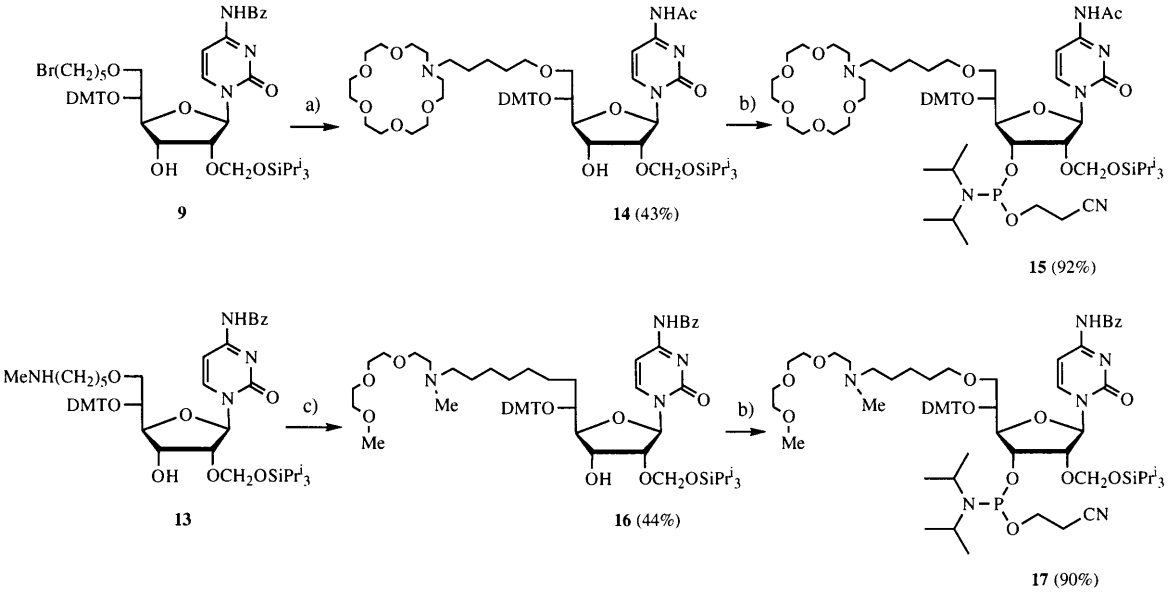

Scheme 2. Reagents and conditions. (a) 1-aza-18-crown-6, Bu_4NI, $Et(Pr^i)_2N$, EtOH, 75°C. (b) (2-cyanoethyl)(*N*,*N*-diisopropylamino)-chlorophosphite, $Et(Pr^i)_2N$, CH_2Cl_2, room temperature. (c) $Me(OCH_2CH_2)_3Cl$, Bu_4NI, $Et(Pr^i)_2N$, toluene, 95°C.

silylation of **2** with triisopropylsilyl triflate, cleavage of the ketal group with 50% trifluoroacetic acid and dibenzoylation with benzoyl chloride. The *N*-allyloxycarbonyl-protected methylaminopentyl sugar **4** was obtained by silylation of **2** with triisopropylsilyl triflate, substitution of bromide (and cleavage of the 3-*O*-benzoyl group) with methylamine, selective *N*-acylation with allyl chloroformate, cleavage of the ketal group and perbenzoylation. Nucleosidation of **3** and **4** was achieved under Vorbrüggen conditions (13) with *in situ* trimethylsilylated N^4-benzoylcytosine using trimethylsilyl triflate (with **3** and **4**) or $SnCl_4$ (with **3**) as Lewis acid. Without isolation of the nucleosidation products the Pr^i_3Si groups were removed with a mixture of aqueous HF and HCl in MeCN and nucleosides **5** and **6** were isolated in good yields. From these the dimethoxytritylated diols **7** and **8** were obtained in excellent yields by treatment with dimethoxytrityl chloride in the presence of collidine and $AgNO_3$ according to Hakimelahi *et al.* (14), directly followed by *O*-debenzoylation.

Regioselective introduction of the $Pr^i_3SiOCH_2$ (TOM) group at the 2′-*O* positions of diols **7** and **8** was carried out under conditions developed in our laboratory (11; S.Pitsch, X.Wu, P.A.Weiss, S.Vonhoff and L.Jenny, in preparation) and gave compounds **9** and **11** in satisfactory yields. The 3′-*O*-alkylated

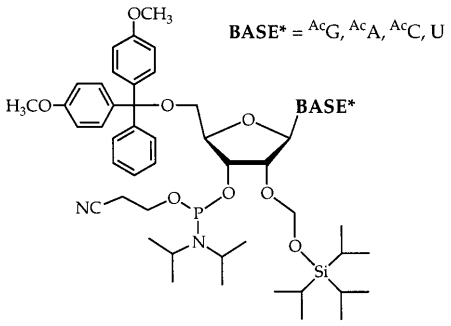

Figure 1. Structure of TOM-protected phosphoramidites (TOM, triisopropylsilyloxymethyl).

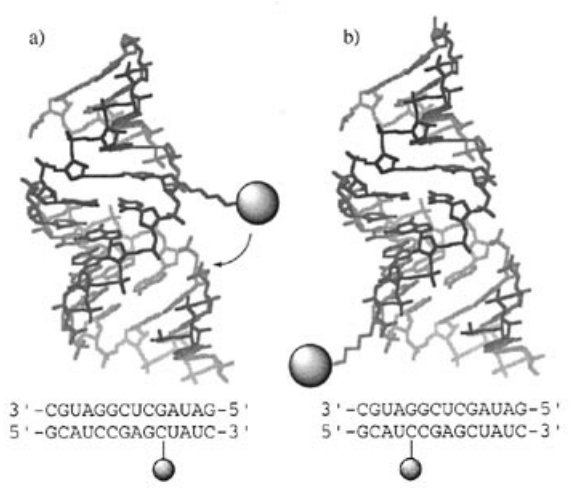

Figure 2. Pictures of modified A-type RNA duplexes, illustrating the position of the additional substituents present in functionalized allofuranosyl nucleosides. (**a**) The internally functionalized duplexes **C**·**A** and **E**·**A**; (**b**) the externally substituted duplexes **D**·**A** and **F**·**A**. Potentially, the functional group attached to oligonucleotides **C** and **E** can reach over the major groove and interact with the other strand (as indicated by the arrow). The RNA duplex was constructed with MacroModel and the substituents were added without further minimization.

regioisomers **10** and **12** were isolated as minor products. Both pairs of regioisomers were unambigously identified by their ^{1}H NMR spectra according to Pitsch (11). From **11** the free methyl aminopentyl nucleoside **13** was obtained according to Hayakawa *et al*. (15).

Functionalization

Reaction of the bromopentyl-substituted nucleoside **9** and 1-aza-6-crown-18 led to the corresponding crown ether-substituted nucleoside. During this reaction partial loss of the benzoyl base-protecting group was observed. Therefore, it was completely removed with ammonia, protected again with Ac_2O and isolated as the N^4-acetylcytosine derivative **14** in fair yield. Under standard conditions, it was finally transformed into phosphoramidite **15** (Scheme 2).

Reaction of the methyl aminopentyl nucleoside **13** and diethyleneglycol monomethyl monochloroethyl diether $CH_3(OCH_2CH_2)_3Cl$ led to the corresponding triethyleneglycol-substituted nucleoside **16**, which was finally transformed into phosphoramidite **17** (Scheme 2).

Synthesis of oligonucleotides

For our initial hybridization studies we designed a non-self-complementary tetradecamer RNA sequence in which we incorporated phosphoramidites **15** and **17** at two different positions, one near the 3′- and one near the 5′-end (Table 1 and Fig. 2). The syntheses were carried out on a 1.5 µmol scale using the conditions in Table 1. Phosphoramidites **15** and **17** were efficiently incorporated (coupling yield >98%) using twice the coupling time required for standard, TOM-protected phosphoramidites (Fig. 1). The removal of base and phosphate protecting groups and cleavage from the solid support was carried out with 10 M $MeNH_2$ in EtOH/H_2O 1:1 at 25°C for 2 h. After evaporation, complete removal of all TOM protecting groups was achieved with 1 M $Bu_4NF{\cdot}3H_2O$ in THF at 25°C for 12 h. After work-up and desalting on Sephadex G-10, the sequences were purified by reversed phase HPLC and characterized by MALDI-TOF mass spectrometry according to Pieles *et al*. (16) (Table 1).

Table 1. The oligonucleotides were prepared under the following conditions

Sequence **X**: from **15** **Y**: from **17**	Isolated yield [%]	MALDI-TOF MS $[M-H^+]^-$ Calc.	 Found
A r(GAUAGCUCGGAUGC)	25	4486	4490
B r(GCAUCCGAGCUAUC)	27	4403	4403
C r(GCAUCCGAG**X**UAUC)	21	4767	4767
D r(GCAU**X**CGAGCUAUC)	18	4767	4767
E r(GCAUCCGAG**Y**UAUC)	15	4681	4682
F r(GCAU**Y**CGAGCUAUC)	16	4681	4682

Detritylation with 4% dichloroacetic acid, 1.2 min for TOM-protected phosphoramidites, 2 min for **15** and **17**; coupling catalysed by 5-benzylthio-1*H*-tetrazole (0.25 M × 360 µl), 2.5 min for TOM-protected phosphoramidites (0.1 M × 120 µl), 5 min for **15** and **17** (0.12 M × 120 µl); capping, Ac_2O/2,6-lutidine/THF (1:1:8), *N*-methylimidazole (16% v/v) in THF (1:1) 2 min; oxidation, I_2/H_2O/pyridine/THF (3:2:20:75) 0.5 min.

Pairing properties

Figure 2 illustrates the position of the metal-binding sites within duplexes formed by the functionalized tetradecamers **C–F** and the corresponding complementary sequence **A**. When the modified nucleosides are near the 3′-end of the sequence (Fig. 2a), they were located in the center of the duplex and the tethered functional groups could reach over the major groove to interact with the backbone of the other strand (duplexes **C**·**A** and **E**·**A**, which are internally functionalized). When the modified nucleosides are near the 5′-end of the sequence (Fig. 2b), the functional groups were located outside the duplex and not able to reach the other strand (duplexes **D**·**A** and **F**·**A**, which are externally functionalized).

We expected that an eventual positive interaction between the two pairing strands would lead to stabilization of the internally functionalized duplexes, but not of the externally functionalized ones. Therefore, the latter were prepared and investigated as

Table 2. Data obtained from measurements in 10 mM Tris–HCl (pH 7.4) and 150 mM NaCl, 150 mM KCl or 150 mM NaCl + 2 mM $MgCl_2$

Duplex	Conditions	T_m (1+1 μM) (°C)	ΔH° (kcal/mol)	$T\Delta S°_{37°C}$ (kcal/mol)	$\Delta G°_{37°C}$ (kcal/mol)	$\Delta\Delta G°_{37°C}$ (kcal/mol)
B·A	NaCl	67.5	–123.1	–103.3	–19.8	
	KCl	64.2	–140.9	–119.8	–21.1	
	NaCl+$MgCl_2$	70.8	–162.1	–136.8	–25.3	
C·A	NaCl	63.8	–131.9	–112.0	–19.9	–0.1
	KCl	61.3	–133.3	–113.5	–19.8	+1.3
	NaCl+$MgCl_2$	67.9	–193.1	–166.2	–26.9	–1.6
D·A	NaCl	64.2	–146.6	–125.4	–21.2	–1.4
	KCl	61.3	–138.7	–118.3	–20.4	+0.7
	NaCl+$MgCl_2$	67.1	–151.8	–128.9	–22.9	+2.4
E·A	NaCl	63.4	–163.7	–141.6	–22.1	–2.3
	KCl	61.5	–163.2	–141.8	–21.4	–0.3
	NaCl+$MgCl_2$	68.8	–240.1	–208.3	–31.8	–6.5
F·A	NaCl	63.0	–127.1	–107.8	–19.3	+0.5
	KCl	61.2	–120.1	–101.8	–18.3	+2.8
	NaCl+$MgCl_2$	68.2	–156.2	–132.6	–23.6	+1.7

The thermodynamic data were extracted from concentration-dependent transition curves according to Marky and Breslauer (17). The $\Delta\Delta G°_{37°C}$ values are relative to the change in free energy of the parent duplex **B·A**.

reference compounds to detect intrinsic contributions which are not the result of a specific interaction across the major groove.

Initially, two sets of exploratory experiments were carried out. In the first set, the transition temperatures of all duplexes were determined at pH 7.4, varying the concentrations of NaCl, KCl and NaCl + $MgCl_2$. In the second set, transition temperatures were determined in 150 mM NaCl + 2 mM $MgCl_2$, varying the pH values from 5 to 9. These measurements revealed no significant differences among the relative duplex stabilities within the covered range of conditions. Further investigations were therefore performed under physiological conditions.

The thermodynamic stability of each duplex was determined at pH 7.4 in the presence of 150 mM NaCl, 150 mM KCl and 150 mM NaCl + 2 mM $MgCl_2$. The results in Table 2 were obtained from concentration-dependent transition temperatures according to the method developed by Marky and Breslauer (17), which allows the determination of $\Delta H°$ and $\Delta S°$ for the pairing process. From these parameters the $\Delta G°$ of duplex formation at a given temperature is calculated according to $\Delta G°(T) = \Delta H° - T\Delta S°$.

The transition temperatures ('melting points') of the duplexes formed from the functionalized oligoribonucleotides **C**, **D**, **E** and **F** and the complementary partner strand **A** were always lower than those of the corresponding unmodified duplex **B·A**. Usually, lower transition temperatures are taken as an indication of weaker pairing. However, determination of the $\Delta G°$ values of duplex formation revealed that at a physiologically relevant temperature of 37°C some of the functionalized oligonucleotides were in fact more strongly paired than the parent one (Table 2 and Fig. 3).

The thermodynamic data for the crown ether-containing RNA strands in both NaCl and KCl solution at 37°C revealed a less favourable $\Delta G°$ for the internally functionalized duplex **C·A** than for the externally functionalized duplex **D·A**. In KCl solution the duplex **C·A** showed a weaker pairing than the unmodified duplex **B·A**, whereas in NaCl both sequences displayed about the same $\Delta G°$ value. In the presence of 2 mM $MgCl_2$, however, the duplex **C·A** displayed a stronger pairing than the duplex **D·A** and than the parent duplex **B·A**. The more negative $\Delta G°$ value of duplex formation for the functionalized duplex **C·A** (relative to the parent duplex **B·A**) is the consequence of a more favourable $\Delta H°$ term, which below 50°C compensates for the less favourable $\Delta S°$ term (Fig. 3).

The $\Delta G°$ values of duplex formation at 37°C obtained from pairing of the triethyleneglycol-substituted oligoribonucleotides **E·A** and **F·A** indicate a stronger association of sequence **E** compared with sequence **F** in all three environments investigated. In KCl and NaCl solution the difference in $\Delta G°_{37°C}$ values was about –3 kcal/mol in favour of the internally functionalized duplex **E·A**. In the presence of 2 mM $MgCl_2$, however, a very large energy difference of –8 kcal/mol (35% of total at 37°C), again in favour of sequence **E**, was observed. The externally functionalized duplex **F·A** uniformly displayed a weaker pairing than the unmodified duplex **B·A**, whereas the internally functionalized duplex **E·A** showed an equal pairing in KCl (–0.3 kcal/mol), a slightly stronger pairing in NaCl (–2.3 kcal/mol) and a much stronger pairing in NaCl + $MgCl_2$ (–6.5 kcal/mol) than the unmodified duplex **B·A**. Again, the strong stabilization of the functionalized duplex **E·A** (relative to the unfunctionalized duplex **B·A**) is a consequence of a more favourable $\Delta H°$ term which below 65°C compensates for the less favourable $\Delta S°$ term (Fig. 3).

DISCUSSION

These thermodynamic data for duplex stability indicate that in the presence of Mg^{2+} ions pairing is slightly stabilized by a 1-aza-18-crown-6 group and strongly stabilized by a triethyleneglycol group tethered to the 6′-*O* position of an allofuranosyl

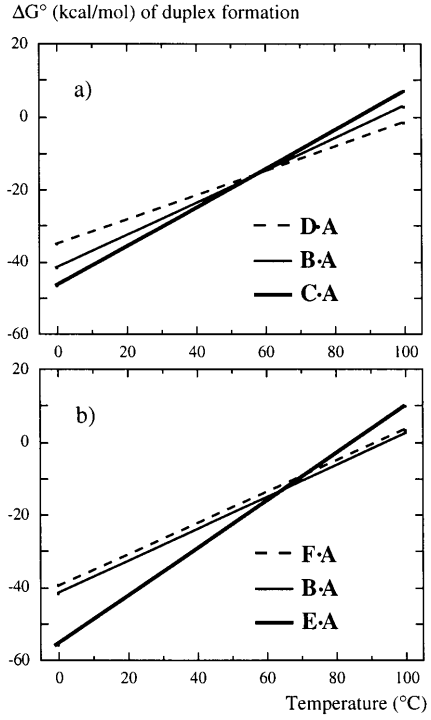

Figure 3. A comparison of the temperature dependance of ΔG° values among the parent duplex **B·A**, the crown ether-substituted duplexes **C·A** and **D·A** (**a**) and the triethylenglycol-substituted duplexes **E·A** and **F·A** (**b**). Data were obtained from concentration-dependant transition curves measured in 150 mM NaCl + 2 mM $MgCl_2$, 10 mM Tris–HCl (pH 7.4).

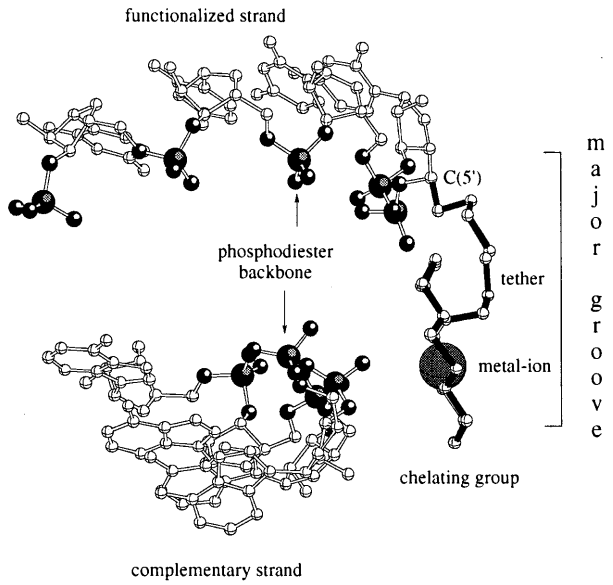

Figure 4. Model representation (MacroModel) of the metal ion-mediated interaction between the two strands of the functionalized duplexes **C·A** and **E·A** as deduced from the thermodynamic data of duplex formation. For the sake of clarity, only the relevant part of the duplex is shown; the atoms of the phosphodiester backbones and the bonds of the functional group are in black.

nucleoside. In the absence of Mg^{2+} ions only the triethyleneglycol-substituted duplex is slightly stabilized.

Structurally, these observations indicate a specific interaction of the Mg^{2+}-complexed ligand of the modified nucleosides with the negatively charged backbone of the other strand. The open chain ligand present in oligonucleotide **E** forms a relatively weak complex with the Mg^{2+} ion, still offering additional coordination sites. It was concluded that the strong duplex stabilization observed results from formation of a complex between the ethyleneglycol moiety, a Mg^{2+} ion and a phosphodiester group of the partner strand **A**. Thereby, one hydrated Mg^{2+} ion within the major groove is replaced by a chelated Mg^{2+} ion (Fig. 4). The cyclic ligand present in oligonucleotide **C** forms a very strong complex with the Mg^{2+} ion and no additional coordination to the phosphodiester backbone is possible. The weak duplex stabilization observed is concluded to be the result of an electrostatic interaction between the positively charged Mg^{2+} complex and the negatively charged phosphodiester backbone of the partner strand.

The additional non-covalent intramolecular interactions were reflected in the enthalpic stabilization of duplexes **C·A** and **E·A**. On the other hand, the conformational changes within the tethered group and/or the backbone required for such an interaction led to an entropic destabilization, which compensated largely, but at low temperature not entirely, for the enthalpic stabilization. In all cases where no stabilization of the duplex could be observed no significant differences in enthalpy and entropy terms were measured, indicating that the additional functional group was pointing into the solution. We were unable to detect any structural changes upon introduction of the functionalized allofuranosyl cytidines into RNA strands by CD spectroscopy. All duplexes essentially had the same CD spectrum, typical for an A-type RNA duplex.

CONCLUSION AND OUTLOOK

The strategy presented here allows a straightforward preparation of a variety of functionalized oligonucleotides and revealed the 5′-position of nucleosides as a new and promising site for modification, labelling and conjugate formation. The metal-binding derivatives which have been prepared as first examples constitute a new principle for stabilizing oligonucleotide duplexes. We now are preparing reactive allofuranosyl and 2′-deoxyallofuranosyl nucleosides with the other three nucleobases and with different tethers. We will also determine whether 5′-triphosphates derived from those can be incorporated enzymatically into DNA or RNA. Employing nucleotide analogues related to those presented in this paper, we are trying to find oligoribo- and oligodeoxyribonucleotide analogues eventually capable of stabilizing RNA and/or DNA structure, catalysing specific strand scission reactions and enhancing cellular uptake.

MATERIALS AND METHODS

General

Work-up implies distribution of the reaction mixture between CH_2Cl_2 and saturated aqueous $NaHCO_3$ solution, drying of the organic layer with $MgSO_4$, filtration and evaporation of the filtrate. TLC: unless otherwise mentioned, precoated silica gel plates from Macherey & Nagel (exceptionally pre-coated Al_2O_3 plates from Merck), stained by dipping into a solution of 10 ml anisaldehyde, 10 ml concentrated H_2SO_4, 2 ml AcOH in 180 ml EtOH and subsequent heating with a heat gun. Column chromatography (CC): unless otherwise mentioned, silica gel 60 (230–400 mesh) from Fluka (exceptionally Al_2O_3, activity III, from ICN Adsorbentien).

Optical rotation ($[\alpha]_D^{25}$): Jasco-DIP-370, all measurements in $CHCl_3$ (1 g/100 ml). UV spectra: Uvikon 931, λ_{max} in nm, ε (dm^3/mol/cm) indicated in parentheses, all measurements in MeOH. NMR: Varian-Gemini 300 (^1H, 300 MHz; ^{31}P, 121 MHz), chemical shift δ_H in p.p.m. (Me_4Si as internal standard), δ_P in p.p.m. (85% H_3PO_4 as external standard), all measurements in $CDCl_3$, coupling constants *J* in Hz. MS: VG-ZAB2-SEQ, all samples measured in FAB^+ mode, 3-nitrobenzyl alcohol as matrix, relative intensity in % as indicated in parentheses.

Oligonucleotide synthesis

The oligoribonucleotides were assembled on CPG supports (1.5 µmol scale) on a Pharmacia Gene Assembler using the methods in Table 1. The TOM-protected phosphoramidites and solid supports were from Xeragon AG (Switzerland). Average coupling yields were >99% (detritylation assay). Deprotection was carried out as described in the text. The crude product was purified by reversed phase HPLC and finally desalted according to Pitsch (11).

Thermal denaturation studies

Absorbance versus temperature profiles were recorded in fused quartz cuvettes at 260 nm on a Cary Bio-1 spectrophotometer equipped with a Peltier temperature control device. The samples were prepared under sterile conditions from stock solutions of the oligonucleotide, 1 M Tris–HCl buffer (pH 7.4) and 5 M NaCl solution and subsequently degassed. A layer of silicon oil was placed on the surface of the solution. The studies were carried out at 0.5, 1, 2, 4 and 8 µM concentrations of both strands. Prior to the measurements, each sample was briefly heated to 80°C. The curves were obtained with both a cooling and heating ramp of 0.3°C/min.

The transition temperatures were obtained after differentiation of the melting curves and analysed according to Marky and Breslauer (17).

3-*O*-Benzoyl-6-*O*-(5-bromopentyl)-1,2-*O*-isopropyliden-α-D-allofuranose (2)

In a Dean-Stark apparatus, a solution of 3-*O*-benzoyl-1,2-*O*-isopropylidene-α-D-allofuranose (**1**) (11) (9.72 g, 30 mmol) and Bu_2SnO (11.2 g, 33 mmol) in toluene (75 ml) was refluxed for 1 h. The toluene was evaporated, the residue diluted with DMF (75 ml) and treated with CsF (6.84 g, 45 mmol), 1,5-dibromopentane (16.3 ml, 120 mmol) and Bu_4NI (16.62 g, 45 mmol). The suspension was kept at room temperature for 8 h. Work-up and CC (hexane/EtOAc 9:1–6:4) gave **2** (9.4 g, 74%) as a colourless, viscous liquid. TLC (hexane/EtOAc 1:1) 0.64; $[\alpha]_D^{25}$ +28.0; δ_H 1.33 (s, Me), 1.41–1.49 (m, CH_2), 1.54 (s, Me), 1.58–1.61 (m, CH_2), 1.81–1.85 (m, CH_2), 2.46 (d, *J* 3.7, 5-OH), 3.37 (t, *J* 6.8, CH_2), 3.40–3.50 (3 H, m, CH_2O, H,H′-6), 4.12 (m, H-5), 4.36 (dd, *J* 3.7, 8.4, H-4), 4.97 (dd, *J* 3.7, 5.0, H-2), 5.15 (dd, *J* 5.0, 8.4, H-3), 5.89 (d, *J* 3.7, H-1), 7.46 (m, 2 ArH), 7.59 (m, 1 ArH); 8.06 (m, 2 ArH); *m/z* 474 (1, MH^+), 104 (100).

6-*O*-(5-bromopentyl)-1,2,3-*O*-tribenzoyl-5-*O*-[(triisopropyl)-silyl]-α,β-D-allofuranose [3(α/β)]

At room temperature, a solution of **2** (3.52 g, 7.4 mmol) in CH_2Cl_2 (25 ml) was treated with Pr^i_2NEt (3.8 ml, 22.2 mmol) and $Pr^i_3SiOSO_2CF_3$ (2.6 ml, 9.7 mmol) for 1 h. After work-up, the crude product was treated with CF_3COOH (50 ml) and H_2O (50 ml) for 2 h. Work-up gave a colourless oil, which was dissolved in pyridine (3 ml) and CH_2Cl_2 (6 ml) and treated with benzoyl chloride (1.5 ml, 13 mmol) and dimethylamino pyridine (82 mg, 0.67 mmol) for 12 h. Work-up and CC (hexane/EtOAc 9:1–7:3) gave **3a**(α/β) (4.7 g, 54%, α/β 1:2 by NMR) as a colourless foam. TLC (hexane/EtOAc 4:1) 0.66; δ_H 0.66–1.15 (21 H, m, Pr^i_3Si), 1.33–1.53 (m, 2 CH_2), 1.65–1.82 (m, CH_2), 3.21–3.24 (m, H-6), 3.34–3.46 (3 H, m, H′-6, CH_2), 3.50–3.62 (m, CH_2), 4.30 [m, H–C(5)], 4.67 [dd, *J* 4.4, 5.6, H-4(α)], 4.97 [m, H-4(β)], 5.60 [dd, *J* 4.4, 6.5, H-2(β)], 5.90 [dd, *J* 2.2, 5.3, H-2(α)], 6.03 [dd, *J* 5.3, 5.5, H-3(α)], 6.09 [dd, *J* 1.9, 6.5, H-3(β)], 6.61 [d, *J* 2.2, H-1(α)], 6.87 [d, *J* 4.4, H-1(β)], 7.17–7.61 (m, 9 ArH), 7.76–8.10 (m, 6 ArH); *m/z* 801 (6, MH^+).

*N*⁴-Benzoyl-1-[6′-*O*-(5-bromopentyl)-2′,3′-di-*O*-benzoyl-β-D-allofuranosyl]cytosine (5)

A suspension of **3**(α/β) (5.4 g, 6.75 mmol), *N*⁴-benzoylcytosine (18) (1.6 g, 7.4 mmol) and bis(trimethylsilyl)acetamide (4.2 ml, 16.9 mmol) in CH_3CN (27 ml) was stirred at 70°C for 1 h, treated with $SnCl_4$ (3.2 ml, 27 mmol) and stirred at 70°C for 20 min. After work-up, the residue was dissolved in CH_3CN (200 ml), treated with HCl (conc.) (2 ml) and HF (40% in H_2O) (4 ml) and stirred at room temperature for 8 h. Work-up and CC (hexane/EtOAc 8:2–4:6) gave **5** (3.6 g, 71%) as a white foam. TLC (hexane/EtOAc 2:8) 0.55; $[\alpha]_D^{25}$ –97.2; λ_{max} 261 (21 000), 229 (28 900); δ_H 1.44–1.64 (4 H, m, 2 CH_2), 1.75–1.90 (m, CH_2), 3.37 (t, *J* 6.8, CH_2), 3.48–3.53 (m, 2 H-6′), 3.65–3.67 (3 H, m, OCH_2, OH-5′), 4.30 (m, H-5′), 4.45–4.49 [m, H–C(4′)], 5.88 (dd, *J* 5.6, 6.6, H-2′), 5.99 (dd, *J* 2.5, 5.6, H-3′), 6.58 (d, *J* 6.8, H-1′), 7.26–8.03 (m, 15 ArH, H-5), 8.35 (d, *J* 7.8, H-6), 8.77 (s, NH); *m/z* 736 (11, M^+).

*N*⁴-Benzoyl-1-[6′-*O*-(5-bromopentyl)-5′-*O*-(4,4′-dimethoxytrityl)-β-D-allofuranosyl]cytosine (7)

A suspension of **5** (2.7 g, 3.6 mmol), $AgNO_3$ (612 mg, 3.6 mmol) and *sym*-collidine (1.2 ml, 9 mmol) in CH_2Cl_2 (12 ml) was treated with 4,4′-dimethoxytrityl chloride (1.84 g, 5.4 mmol) for 1 h at room temperature. After filtration and evaporation, the residue was dissolved in an ice-cold solution of THF/MeOH/H_2O 5:4:1 (150 ml), treated with 10 N aqueous NaOH (3 ml) at 4°C for 15 min, then neutralized with AcOH (1.9 ml) and concentrated to 40 ml. Work-up and CC [CH_2Cl_2 to CH_2Cl_2/MeOH 97:3 (+2% NEt_3)] gave **7** (2.46 g, 84%) as a white foam. TLC (MeOH/CH_2Cl_2 8:92) 0.50; $[\alpha]_D^{25}$ +28.4; λ_{max} 262 (14 700), 238 (22 300); δ_H 1.44–1.63 (m, 2 CH_2), 1.80–1.92 (m, CH_2), 3.19–3.27 (m, OCH_2, H-6′), 3.42 (t, *J* 6.5, CH_2), 3.40–3.45 (m, H′-6′), 3.55–3.64 (m, H-5′, OH), 3.80 (s, 2 OMe), 4.21–4.27 (m, H-2′, H-4′), 4.44 (s, OH), 4.67 (dd, *J* 5.6, 5.8, H-3′), 5.86 (d, *J* 3.1, H-1′), 6.82–6.86 (m, 4 ArH), 7.22–7.63 (m, 12 ArH, H-5), 7.88–7.89 (m, 2 ArH), 7.92 (d, *J* 7.5, H-6), 8.88 (s, NH); *m/z* 829 (18, MH^+), 303 (100).

*N*⁴-Benzoyl-1-[6′-*O*-(5-bromopentyl)-5′-*O*-(4,4′-dimethoxytrityl)-2′-*O*-{[(triisopropyl)silyloxy]methyl}-β-D-allofuranosyl]cytosine (9)

A solution of **7** (2.46 g, 3.0 mmol) and Pr^i_2NEt (2.1 ml, 12 mmol) in $ClCH_2CH_2Cl$ (10 ml) was treated with Bu_2SnCl_2 (1.1 g,

3.6 mmol) at room temperature for 1.5 h, then treated with $Pr^i_3SiOCH_2Cl$ (1.0 g, 4.5 mmol) at 80°C for 15 min. Work-up and CC [hexane/EtOAc 5:5–2:8 (+ 2% NEt_3)] gave **9** (1.28 g, 42%) and **10** (570 mg, 20%) as pale yellow foams. TLC (hexane/EtOAc 3:7) 0.63; $[\alpha]_D^{25}$ +36.8; λ_{max} 260 (17 800), 238 (23 800); δ_H 1.08–1.22 (21 H, m, Pr^i_3Si), 1.41–1.49 (m, 2 CH_2), 1.81–1.86 (m, CH_2), 3.15–3.22 (m, H-6′, CH_2O), 3.39 (t, *J* 6.9, CH_2), 3.50–3.55 (m, OH, H′-6′), 3.67 (s, H-5′), 3.81 (s, 2 OMe), 4.15–4.20 (m, H-2′, H-4′), 4.63 (dd, *J* 5.4, 6.4, H-3′), 5.11 and 5.23 (2d, *J* 4.7, OCH_2O), 6.01 (d, *J* 2.8, H-1′), 6.84–6.87 (m, 4 ArH), 7.25–7.61 (m, 12 ArH, H-5), 7.79–7.88 (m, 2 ArH), 7.89 (d, *J* 7.8, H-6), 8.61 (s, NH); *m*/*z* 1016 (100, MH^+).

N^4-Benzoyl-1-[6′-*O*-(5-bromopentyl)-5′-*O*-(4,4′-dimethoxytrityl)-3′-*O*-{[(triisopropyl)silyloxy]methyl}-β-D-allofuranosyl]-cytosine (10)

From the reaction described above. TLC (hexane/EtOAc 3:7) 0.35; $[\alpha]_D^{25}$ –11.4; δ_H 1.08–1.11 (21 H, m, Pr^i_3Si), 1.39–1.48 (m, 2 CH_2), 1.81–1.86 (m, CH_2), 3.13–3.21 (m, H-6′, OCH_2), 3.40 (t, *J* 6.8, CH_2), 3.37–3.42 (m, H′-6′), 3.50 (s, H-5′), 3.80 (s, 2 OMe), 3.77–3.84 (m, OH-2′), 4.12 (m, H-2′), 4.32 (m, H-4′), 4.65 (dd, *J* 3.4, 5.6, H-3′), 4.98 and 5.17 (2d, *J* 4.8, OCH_2O), 5.96 (d, *J* 6.2, H-1′), 6.83–6.85 (m, 4 ArH), 7.23–7.62 (m, 14 ArH, H-5), 7.90 (d, *J* 7.2, H-6), 8.61 (s, NH); *m*/*z* 1016 (54, MH^+), 303 (100).

N^4-Acetyl-1-{6′-*O*-[5-(1,4,7,10,13-pentaoxa-16-aza-cyclooctadec-16-yl)-pentyl]-5′-*O*-(4,4′-dimethoxytrityl)-2′-*O*-{[(triisopropyl)silyloxy]methyl}-β-D-allofuranosyl}cytosine (14)

A solution of **9** (408 mg, 0.4 mmol), 1-aza-18-crown-6 (263 mg, 1.0 mmol), Pr^i_2NEt (0.34 ml, 2 mmol) and Bu_4NI (222 mg, 0.6 mmol) in EtOH (1 ml) was stirred at 75°C for 30 h. After work-up, the residue was treated with NH_3 in EtOH/H_2O 9:1 (2 ml) at room temperature for 10 h. Evaporation and filtration through a short Al_2O_3 column (CH_2Cl_2/MeOH 9:1) gave a product (277 mg, 0.25 mmol) which was dissolved in DMF (1 ml) and treated with Ac_2O (31 µl, 0.32 mmol). After stirring for 4 h at room temperature, work-up and CC (Al_2O_3, CH_2Cl_2 to MeOH/CH_2Cl_2 3:97) **14** (192 mg, 43%) was obtained as a yellow foam. TLC (Al_2O_3, MeOH-CH_2Cl_2 4:96) 0.42; $[\alpha]_D^{25}$ +19.9; λ_{max} 261 (19 900), 238 (23 600); δ_H 1.06–1.09 (21 H, m, Pr^i_3Si), 1.20–1.28 (m, CH_2), 1.37–1.49 (m, 2 CH_2), 2.21 (s, MeCO), 2.46 (t, *J* 7.5, CH_2), 2.74 (t, *J* 5.9, 4 CH_2), 3.12–3.19 (m, H-6′, CH_2O), 3.45–3.50 (dd, *J* 6.5, 10.5, H′-6′), 3.58–3.67 (22 H, m), 3.80 (s, OMe), 4.12–4.15 (m, H-2′, H-4′), 4.60 (m, H-3′), 5.07 and 5.21 (2d, *J* 4.7, OCH_2O), 5.98 (d, *J* 3.8, H-1′), 6.81–6.84 (m, 4 ArH), 7.23–7.51 (m, ArH, H-5), 7.74–7.67 (d, *J* 7.5, H-6), 9.18 (s, NH); *m*/*z* 1136 (100, M^+).

N^4-Acetyl-1-{6′-*O*-[5-(1,4,7,10,13-pentaoxa-16-aza-cyclooctadec-16-yl)-pentyl]-5′-*O*-(4,4′-dimethoxytrityl)-2′-*O*-{[(triisopropyl)silyloxy]methyl}-β-D-allofuranosyl}cytosine 3′-[(2-cyanoethyl) *N*,*N*-diisopropyl-phosphoramidite] (15)

A solution of **14** (192 mg, 0.17 mmol) in CH_2Cl_2 (0.75 ml) was treated consecutively with Pr^i_2NEt (73 µl, 0.43 mmol) and (2-cyanoethyl)(*N*,*N*-diisopropylamino)chlorophosphite (48 mg, 0.20 mmol). After stirring for 1 h at room temperature, the mixture was subjected to CC (Alox, hexane/EtOAc 6:4–3:7) and **15** (210 mg, 92%) was obtained as a pale yellow foam (1:1 mixture of diastereoisomers). TLC (Al_2O_3, MeOH/CH_2Cl_2 4:96) 0.52; λ_{max} 239 (23 600); δ_H 1.00–1.07 (21 H, m, Pr^i_3Si), 1.13–1.21 (m, 4 Me), 1.32–1.36 (m, 3 CH_2), 2.21 (s, MeCO), 2.42–2.44 (m, CH_2), 2.54 and 2.61 (2t, *J* 6.5, CH_2), 2.73 (t, *J* 5.8, 4 CH_2), 2.97–3.08 (m, OCH_2, H-6′), 3.39–3.67 (25 H, m), 3.79 (s, 2 OMe), 4.27 and 4.32 (2dd, *J* 5.0, 5.3, H-2′), 4.40 (m, H-4′), 4.64–4.77 (m, H-3′), 4.96–5.06 (m, OCH_2O), 6.05 (0.5 H, d, *J* 3.7, H-1′), 6.06 (0.5 H, d, *J* 4.7, H-1′), 6.81–6.84 (m, 4 ArH), 7.23–7.50 (m, 10 ArH, H-5), 7.61–7.66 (m, H-6), 9.18 (s, NH); δ_P 150.2, 149.8; *m*/*z* 1336 (100, M^+).

6-*O*-[5-(*N*-Allyloxycarbonyl-methylamino)-pentyl]-1,2,3-tri-*O*-benzoyl-5-*O*-[(triisopropyl)silyl]-β-D-allofuranose [4(α/β)]

At room temperature, a solution of **2** (9.78 g, 21 mmol) in CH_2Cl_2 (70 ml) was treated with Pr^i_2NEt (10.8 ml, 63 mmol) and $Pr^i_3SiOSO_2CF_3$ (7.34 ml, 27.3 mmol) for 1 h. Work-up gave a crude product, which was treated with $MeNH_2$ in EtOH (8 M, 70 ml) for 1 h at room temperature. After evaporation and work-up, the residue was dissolved in CH_2Cl_2 (70 ml) and treated with Pr^i_2NEt (7.2 ml, 42 mmol) and allyl chloroformate (2.2 ml, 21 mmol) at room temperature for 0.5 h. Work-up gave a yellow oil. The crude product obtained by treatment of the resulting oil with CF_3COOH (50 ml) and H_2O (50 ml) for 1 h at room temperature was dissolved in pyridine (15 ml) and CH_2Cl_2 (30 ml) and treated with benzoyl chloride (5.6 ml, 48 mmol) and dimethylaminopyridine (293 mg, 2.4 mmol) for 12 h. Work-up and CC (hexane/EtOAc 9:1–7:3) gave **4**(α/β) (2.5 g, 42%, α/β 1:2 by ^1H NMR). TLC (hexane/EtOAc 7:3) 0.47; δ_H 1.05–1.15 (7 H, m, Pr^i_3Si), 1.21 (m, CH_2), 1.44 (m, 2 CH_2), 2.83 (s, CH_3), 3.09–3.11 (m, CH_2), 3.31–3.41 (m, 2 H-6), 3.59 (d, *J* 5.9, CH_2), 4.26 [m, H-5(α)], 4.31 [m, H-5(β)], 4.55 (m, CH_2), 4.66 [dd, *J* 4.3, 5.1, H-4(α)], 4.78 [dd, *J* 1.8, 1.9, H-4(β)], 5.23 (m, CH_2), 5.60 [dd, *J* 4.3, 6.5, H-2(β)], 5.90 [dd, *J* 2.5, 5.3, H-2(α)], 5.92–5.94 (m, CH), 6.02 [dd, *J* 2.2, 5.3, H-3(α)], 6.08 [dd, *J* 1.9, 6.5, H-3(β)], 6.61 [d, *J* 2.1, H-1(α)], 6.87 [d, *J* 4.4, H-1(β)], 7.17–7.61 (m, 9 ArH), 7.75–8.12 (m, 6 ArH); *m*/*z* 833 (2, MH^+), 710 (100).

N^4-Benzoyl-1-{6′-*O*-[5-(*N*-allyloxycarbonyl-methylamino)-pentyl]-2′,3′-di-*O*-benzoyl-β-D-allofuranosyl}cytosine (6)

As described for **5**, with **4**(α/β) (4.7 g, 5.7 mmol), *N*^{4}-benzoyl-cytosine (18) (1.36 g, 6.3 mmol), bis(trimethylsilyl)acetamide (3.5 ml, 14.4 mmol), CH_3CN (20 ml), Me_3Si-OTf (2.7 ml, 22.8 mmol), then CH_3CN (100 ml), HCl (conc.) (1 ml), HF (40% in H_2O) (2 ml). Work-up and CC (hexane/EtOAc 8:2–4:6) gave **6** (3.4 g, 74%) as a white foam. TLC (hexane/EtOAc 4:6) 0.53; $[\alpha]_D^{25}$ –54.2; λ_{max} 261 (26 600), 237 (30 100); δ_H 1.34 (m, CH_2), 1.57 (m, 2 CH_2), 2.89 (s, CH_3), 3.26 (br. s, CH_2), 3.51–3.53 (m, 2 H-6′), 3.64–3.66 (m, CH_2O, OH), 4.29 (s, H-5′), 4.45 (s, H-4′), 4.57–4.59 (m, CH_2), 5.25 (m, CH_2), 5.83–5.97 (m, H-2′, H-3′, CH), 6.60 (s, H-1′), 7.27–8.03 (m, 15 ArH, H-5), 8.36 (m, H-6), 8.72 (s, NH); *m*/*z* 770 (100, MH^+).

N^4-Benzoyl-1-{6′-*O*-[5-(*N*-allyloxycarbonyl-methylamino)-pentyl]-5′-*O*-(4,4′-dimethoxytrityl)-β-D-allofuranosyl}cytosine (8)

As described for **7**, with **6** (2 g, 2.66 mmol), $AgNO_3$ (687 mg, 4.0 mmol), *sym*-collidine (0.7 ml, 2 mmol), CH_2Cl_2 (12 ml), 4,4′-dimethoxytrityl chloride (1.36 g, 4.0 mmol), then THF/

MeOH/H_2O 5:4:1 (120 ml), 10 N aqueous NaOH (2.4 ml), AcOH (1.5 ml). Work-up and CC [CH_2Cl_2 to CH_2Cl_2/MeOH 98:2 (+2% NEt_3)] gave **8** (2.1 g, 91%) as a white foam. TLC (MeOH/CH_2Cl_2 8:92) 0.54; $[\alpha]_D^{25}$ +28.3; λ_{max} 258 (13 400), 237 (27 000); δ_H 1.27 (m, CH_2), 1.32 (m, 2 CH_2), 2.90 (s, CH_3), 3.21–3.30 (m, CH_2, CH_2O, H-6′), 3.41 (dd, *J* 4.2, 10.5, H′-6′), 3.62 (s, H-5′), 3.80 (s, 2 OMe), 4.22 (m, H-2′, H-4′), 4.56 (d, *J* 5.3, CH_2), 4.66 (m, H-3′), 5.16–5.30 (m, CH_2), 5.88 (d, *J* 2.2, H-1′), 5.89–5.97 (m, CH), 6.82–6.85 (m, 4 ArH), 7.21–7.62 (m, 12 ArH, H-5), 7.88–7.93 (m, 2 ArH, H-6), 8.65 (s, NH); *m/z* 864 (28, MH^+), 303 (100).

N^4-Benzoyl-1-{6′-*O*-[5-(*N*-allyloxycarbonyl-methylamino)-pentyl]-5′-*O*-(4,4′-dimethoxytrityl)-2′-*O*-{[(triisopropyl)silyl-oxy]methyl}-β-D-allofuranosyl}cytosine (11)

As described for **9,** with **8** (862 mg, 1.0 mmol), Pr^i_2NEt (0.85 ml, 5 mmol), $ClCH_2CH_2Cl$ (4 ml), Bu_2SnCl_2 (340 mg, 1.1 mmol), $Pr^i_3SiOCH_2Cl$ (230 mg, 1.2 mmol). Work-up and CC [hexane/EtOAc 5:5–2:8 (+2% NEt_3)] gave **11** (470 mg, 45%) and **12** (209 mg, 20%) as pale yellow foams. TLC (hexane/EtOAc 15:85) 0.60; $[\alpha]_D^{25}$ +29.1; λ_{max} 260 (23 900), 238 (28 700); δ_H 1.07–1.14 (21 H, m, Pr^i_3Si), 1.23 (m, CH_2), 1.46–1.56 (m, 2 CH_2), 2.89 (s, Me), 3.13–3.26 (m, 2 CH_2, H-6′), 3.48–3.56 (m, OH, H′-6′), 3.64–3.66 (m, H-5′), 3.82 (s, 2 OMe), 4.11 (m, H-2′), 4.20 (m, H-4′), 4.56–4.67 (m, H-3′, CH_2), 5.15 and 5.23 (2d, *J* 4.6, OCH_2O), 5.17–5.31 (m, CH_2), 5.88–5.97 (m, CH), 6.01 (d, *J* 2.3, H-1′), 6.83–6.86 (m, 4 ArH), 7.23–7.63 (m, 12 ArH, H-5), 7.87–7.89 (m, 2 ArH, H-6), 8.57 (s, NH); *m/z* 1050 (4, MH^+), 303 (100).

N^4-Benzoyl-1-{6′-*O*-[5-(*N*-allyloxycarbonyl-*N*-methyl)-pentyl]-5′-*O*-(4,4′-dimethoxytrityl)-3′-*O*-{[(triisopropyl)silyl-oxy]methyl}-β-D-allofuranosyl}cytosine (12)

Obtained from the reaction described above. TLC (hexane/AcOEt 15:85) 0.36; $[\alpha]_D^{25}$ –7.2; λ_{max} 260 (24 600), 238 (29 700); δ_H 1.07–1.11 (21 H, m, Pr^i_3Si), 1.20–1.26 (m, CH_2), 1.42–1.64 (m, 2 CH_2), 2.90 (s, CH_3), 3.22–3.27 (m, NCH_2, CH_2O, H-6′), 3.36–3.41 (m, H′-6′), 3.48–3.50 (m, H-5′), 3.75–3.81 (m, OH-2′), 3.80 (s, 2 OMe), 4.10–4.14 (m, H-2′), 4.32 (m, H-4′), 4.56–4.58 (m, CH_2), 4.65 (m, H-3′), 4.97 and 5.17 (2d, *J* 4.7, OCH_2O), 5.20–5.31 (m, CH_2), 5.89–5.98 (m, CH), 5.96 (d, *J* 6.2, H-1′), 6.79–6.86 (m, 4 ArH), 7.21–7.64 (m, 14 ArH, H-5), 7.90 (d, *J* 6.2, H-6), 8.64 (s, NH); *m/z* 1059 (8, MH^+), 303 (100).

N^4-Benzoyl-1-{6′-*O*-(*N*-methyl-5-aminopentyl)-5′-*O*-(4,4′-dimethoxytrityl)-2′-*O*-{[(triisopropyl)silyloxy]methyl}-β-D-allofuranosyl}cytosine (13)

A suspension of $Pd[P(Ph)_3]_4$ (126 mg, 0.11 mmol) and PPh_3 (60 mg, 0.23 mmol) in CH_2Cl_2 (3 ml) was added dropwise to a solution of **11** (604 mg, 0.58 mmol) and Et_2NH (0.3 ml, 2.9 mmol) in CH_2Cl_2 (3 ml). The solution was stirred for 1 h at room temperature. After evaporation, the residue was subjected to CC [CH_2Cl_2 to MeOH/CH_2Cl_2 5:95 (+ 2% Et_3N)] and **13** (488 mg, 88%) was obtained as a yellow foam. TLC (Al_2O_3, MeOH/CH_2Cl_2 4:96) 0.45; $[\alpha]_D^{25}$ +23.4; λ_{max} 261 (19 800), 238 (25 500); δ_H 1.08 (21 H, m, Pr^i_3Si), 1.29–1.37 (m, CH_2), 1.44–1.51 (m, 2 CH_2), 2.43 (s, NMe), 2.55 (t, *J* 1.2, NCH_2), 3.15–3.20 (m, OCH_2, H-6′), 3.48–3.56 (m, H′-6′, NH), 3.65–3.68 (m, H-5′), 3.77–3.79 (m, OH-3′), 3.81 (s, 2 OMe), 4.13–4.17 (m, H-4′), 4.21 (dd, *J* 3.1, 5.3, H-2′), 4.63–4.65 (m, H-3′), 5.10 and 5.22 (2 d, *J* 4.7, OCH_2O), 5.99 (d, *J* 3.1, H-1′), 6.83–6.86 m, 4 ArH), 7.25–7.63 (m, 12 ArH, H-5), 7.80–7.83 (m, 2 ArH), 7.91 (d, *J* 7.2, H-6); *m/z* 965 (100, M^+).

N^4-Benzoyl-1-{6′-*O*-(*N*-methyl-5-[(2-[2-methoxy-ethoxy]-ethoxy)-ethylamino]-pentyl)-5′-*O*-(4,4′-dimethoxytrityl)-2′-*O*-{[(triisopropyl)silyloxy]methyl}-β-D-allofuranosyl}cytosine (16)

A solution of **13** (244 mg, 0.253 mmol), Bu_4NI (187 mg, 0.506 mmol), Pr^i_2NEt (0.17 ml, 1.0 mmol) in 0.8 ml toluene was treated with $Me(OCH_2CH_2)_3Cl$ (18) (110 mg, 0.61 mmol) and stirred for 8 h at 95°C. Work-up and CC [CH_2Cl_2 to MeOH/CH_2Cl_2 3:97 (+ 2% Et_3N)] gave **16** (120 mg, 44%) as a yellow foam. TLC (Al_2O_3, MeOH/CH_2Cl_2 3:97) 0.41; λ_{max} 259 (19 700), 234 (28 700); δ_H 1.05–1.09 (21 H, m, Pr^i_3Si), 1.26–1.29 (m, CH_2), 1.32–1.39 (m, 2 CH_2), 2.25 (s, NMe), 2.33–2.38 (m, NCH_2), 2.55–2.59 (m, CH_2), 3.14–3.21 (m, OCH_2, H-6′), 3.36 (s, OMe), 3.50–3.66 (m, OH-3′, 2 CH_2, H′-6′, H-5′), 3.80 (s, 2 OMe), 4.14–4.21 (m, H-2′, H-4′), 4.62–4.66 (m, H-3′), 5.13 and 5.23 (2 d, *J* 4.7, OCH_2O), 6.01 (d, *J* 2.8, H-1′), 6.84–6.86 (m, 4 ArH), 7.25–7.63 (m, 12 ArH, H-5), 7.82–7.85 (m, 2 ArH), 7.88 (d, *J* 7.2, H-6); *m/z* 1113 (3, MH^+), 303 (100).

N^4-Benzoyl-1-{6′-*O*-(*N*-methyl-5-[(2-[2-methoxy-ethoxy]-ethoxy)-ethylamino]-pentyl)-5′-*O*-(4,4′-dimethoxytrityl)-2′-*O*-{[(triisopropyl)silyloxy]methyl}-β-D-allofuranosyl}cytosine 3′-[(2-cyanoethyl) *N,N*-diisopropyl-phosphoramidite] (17)

As described for **15**, with **16** (120 mg, 0.11 mmol), CH_2Cl_2 (0.3 ml), Pr^i_2NEt (47 µl, 0.28 mmol) and (2-cyanoethyl)(*N,N*-diisopropylamino)chlorophosphite (31 mg, 0.12 mmol). CC (Al_2O_3, hexane/AcOEt 6:4–2:8) gave **17** (130 mg, 90%) as a pale yellow foam (1:1 mixture of diastereoisomers). TLC (Al_2O_3, MeOH/CH_2Cl_2 4:96) 0.52; λ_{max} 261 (18 700), 239 (27 700); δ_H 1.02–1.08 (21 H, m, Pr^i_3Si), 1.16–1.25 (m, 4 Me), 1.26–1.28 (m, CH_2), 1.34–1.39 (m, 2 CH_2), 2.24 (s, NMe), 2.31–2.34 (m, NCH_2), 2.54–2.63 (m, 2 CH_2), 2.92–3.08 (m, OCH_2, H-6′), 3.36 and 3.37 (2s, CH_3), 3.43–3.62 (m, 12 H, 2 CH_2, H′-6′, H-5′), 3.80 (s, 2 OMe), 4.20–4.41 (m, H-2′, H-4′), 4.66–4.69 (m, 0.5 H, H-3′), 4.75–4.79 (m, 0.5 H, H-3′), 5.00–5.05 (m, OCH_2O), 6.07 and 6.09 (2 s, H-1′), 6.82–6.85 (m, 4 ArH), 7.23–7.71 (m, 12 ArH, H-5), 7.89–7.91 (m, 2 ArH), 8.02 (d, *J* 7.2, H-6), 8.61 (s, NH); δ_P 150.2, 149.8; *m/z* 1313 (26, MH^+), 1312 (36, M^+), 303 (100).

SUPPLEMENTARY MATERIAL

The ^{13}C NMR and IR data of compounds **2**–**17**, the CD spectra of all duplexes and a table of all concentration-dependant transition temperatures are available upon request.

ACKNOWLEDGEMENTS

We thank Prof. A. Vasella for continously supporting this work. We also thank Patrick A. Weiss (Xeragon AG, Switzerland) for providing us with numerous reagents and TOM-phosphoramidites and T. Vivlemore and A. Ernst for helpful suggestions. The ETH Zürich Research Council and the Alfred Werner Foundation are gratefully acknowledged for financial support.

REFERENCES

1 Uhlmann,E. and Peyman,A. (1990) *Chem. Rev.*, **90**, 543–583.
2 Joyce,G.F. (1998) *Proc. Natl Acad. Sci. USA*, **95**, 5845–5847.
3 Allerson,C.C., Chen,S.L. and Verdine,G.L. (1997) *J. Am. Chem. Soc.*, **119**, 7423–7433.
4 De Mesmaeker,A., Häner,R., Martin,P. and Moser,H. (1995) *Acc. Chem. Res.*, **28**, 366–374.
5 Wada,T., Kobayashi,N., Mori,T. and Sekine,M. (1998) *Nucleosides Nucleotides*, **17**, 351–364.
6 Tyagi,S. and Kramer,F.R. (1996) *Nature Biotechnol.*, **14**, 303–308.
7 Pitsch,S. (1997) *Chimia*, **51**, 242–243.
8 Pitsch,S., Wu,X., Weiss,P.A. and Jenny,L. (1998) In Brow,D., Gesteland,R., Krämer,A. and Pyle,A. (eds), *RNA '98: The Third Annual Meeting of the RNA Society, Program & Abstracts*. University of Wisconsin, pp. 554.
9 Vögtle,F. and Weber,E. (1979) *Angew. Chem. Int. Edn English*, **18**, 753–776.
10 Izatt,R.M., Bradshaw,J.S., Nielsen,S.A., Lamb,J.D. and Christensen,J.J. (1985) *Chem. Rev.*, **85**, 271–339.
11 Pitsch,S. (1997) *Helv. Chim. Acta*, **80**, 2286–2314.
12 Nagashima,N. and Ohno,M. (1991) *Chem. Pharm. Bull.*, **39**, 1972–1982.
13 Vorbrüggen,H. and Krolikiewicz,K. (1975) *Angew. Chem.*, **87**, 417.
14 Hakimelahi,G.H., Proba,Z.A. and Ogilvie,K.K. (1982) *Can. J. Chem.*, **60**, 1106–1113.
15 Hayakawa,Y., Hirose,M. and Noyori,R. (1993) *J. Org. Chem.*, **58**, 5551–5555.
16 Pieles,U., Zürcher,W., Schär,M. and Moser,H.E. (1993) *Nucleic Acids Res.*, **21**, 3191–3196.
17 Marky,L.A. and Breslauer,K.J. (1987) *Biopolymers*, **26**, 1601–1620.
18 Brown,D.M., Todd,A.R. and Varadarajan,S. (1956) *J. Chem. Soc.*, 2384–2386.
19 Zellhoefer,G.F. (1937) *Indust. Eng. Chem.*, **29**, 548–550.